Title

ATOMIC MECHANISMS OF PRECIPITATE PLATE GROWTH IN THE Al-Ag SYSTEM - I. CONVENTIONAL TRANSMISSION ELECTRON MICROSCOPY

Authors

Howe, J.M.
Aaronson, H.I.
Gronsky, R.

Publication Date

1984-09-01

Lawrence Berkeley Laboratory
UNIVERSITY OF CALIFORNIA

Materials & Molecular Research Division

Submitted to Acta Metallurgica

ATOMIC MECHANISMS OF PRECIPITATE PLATE GROWTH IN THE Al-Ag SYSTEM - I. CONVENTIONAL TRANSMISSION ELECTRON MICROSCOPY

J.M. Howe, H.I. Aaronson, and R. Gronsky

September 1984

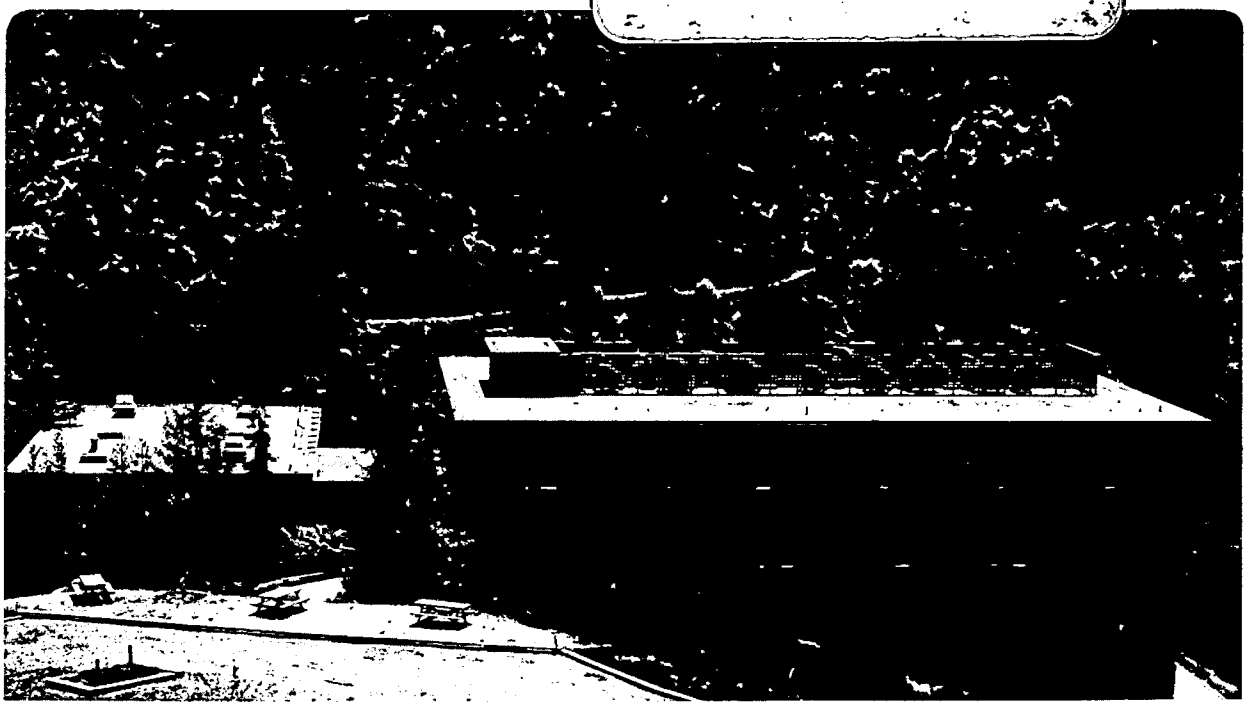

Prepared for the U.S. Department of Energy under Contract DE-AC03-76SF00098

DISCLAIMER

Atomic Mechanisms of Precipitate Plate Growth in the Al-Ag System - I. Conventional Transmission Electron Microscopy

J.M. Howe, H.I. Aaronson* and R. Gronsky

Materials and Molecular Research Division
Lawrence Berkeley Laboratory
Department of Materials Science and Mineral Engineering
University of California, Berkeley, CA 94720

ABSTRACT

The detailed interfacial structure of γ' precipitates in an Al-15 w/o Ag alloy has been studied by conventional transmission electron microscopy. Contrast analyses indicate that there is a strong tendency for single 1/6 <112> Shockley partial dislocations on the precipitate faces to interact, forming multiple-unit ledges which display the contrast behavior of 1/2 <110> dislocations. In addition, both the edges of these precipitates and ledges on the edges are comprised of the same partial dislocations stacked vertically or slightly behind one another. All three variants of Shockley partials have been observed on the same {111} faces of precipitates, and all interfaces of the precipitates display a strong preference for <110> configurations. The similarities between growth of ledges on the broad faces and the edges of precipitates by a kink mechanism are described and explained.

I. INTRODUCTION

The interfacial structure and growth kinetics of γ' and $\gamma(Ag_2Al)$ precipitate plates in Al-Ag alloys have been extensively studied by conventional and "in-situ" transmission electron microscopy (TEM) techniques[1-11] because these precipitates represent one of the simplest diffusional transformations involving a distinct change in crystal

structure, i.e. from fcc to hcp.[12] This system also serves as an ideal model with which to test the "general theory of precipitate morphology" originally proposed by Aaronson[13] in 1962, and which has been explored in many previous publications.[4,8,14-26] According to this theory, when the composition and crystal structure of a precipitate differ from that of the matrix, the precipitate morphology is determined by the mechanism of atomic attachment across the interphase boundary. In the case of precipitate plates, the edges or fast-growing faces of these plates are proposed to have high-energy disordered structures, permitting them to grow at a rate limited only by nonstructural factors such as long-range volume diffusion. Conversely, the broad faces or slow-growing faces of these plates are proposed to have lower-energy ordered (coherent or semicoherent) structures requiring them to grow only by the formation and passage of ledges laterally across the interphase boundary. Although the edges of such ledges could have a disordered structure and therefore also move at a rate controlled by volume diffusion, the ledge mechanism of growth is overall a much slower process, which results in a large aspect ratio, as observed for plate morphologies.

Within about the last 20 years, the growth behavior of the faces and edges of plate-shaped precipitates in a variety of alloy systems has been compared to growth kinetics predicted for fully or partially coherent and disordered interfaces.[27-46] While these studies have mostly confirmed the predictions of the general theory of precipitate growth, several contrary results have been obtained,[24] and the theory has not gone unchallenged.[19-23,25] For instance, in the Al-Ag system

chosen for this study, hot-stage TEM and kinetic analyses[8] now indicate that both the faces and edges of $\gamma(Ag_2Al)$ precipitates may grow by a ledge mechanism and therefore, that the precipitates may be fully or partially coherent in a number of different boundary orientations, not just at their faces. Hence, it has been further proposed that the morphology might depend on factors such as interledge spacing versus boundary orientation.[16] These same analyses also showed that the heights and growth behavior of ledges or "superledges" on the plate edges are considerably different from those on the faces of the precipitates, and that the growth rate of individual ledges on the faces are sometimes much slower than allowed by volume diffusion, suggesting that they are actually several ledges high or alternatively, that a kink-on-ledge mechanism of growth was necessary to effect movement. In addition, there has been some dispute as to whether this ledge mechanism or interfacial energy effects are responsible for the large aspect ratios of these precipitates.[19-24]

While this new information questions the validity of disordered interphase boundaries as previously envisioned, almost all of the recent work in this area has concentrated on theoretical modeling of the growth process using computer simulations.[47,48] Although these studies have yielded valuable insight into possible growth behavior of both individual ledges and the edges of precipitate plates, there have not been any new TEM investigations of the structural aspects of this phenomenon in the Al-Ag system since the original studies performed in the 1960's. Marked improvements in both the technique and instrumentation aspects of TEM which have appeared since then warrent further investigation

of precipitation processes in Al-Ag alloys in order to seek better answers to problems remaining incompletely resolved. Therefore, complementary conventional and high-resolution TEM studies were undertaken for the specific purpose of obtaining detailed structural information about the heights and character of ledges on both the faces and edges of precipitate plates. This information will be used to test further the general theory of precipitate morphology and also the predictions of subsequent theoretical models on a more nearly atomic level. This article reports the results of the conventional TEM studies.

2. EXPERIMENTAL PROCEDURES

2.1 Material

An Al-14.92 w/o Ag (4.2 a/o Ag) alloy was vacuum melted and cast, using Al and Ag of 99.99% purity. The ingot was homogenized at 535° C for about 40 hours to reduce segregation, and then hot and cold rolled to 7 mil (25μm) final thickness.

2.2 Heat Treatment

The microstructures resulting from two different heat treatments were examined in this study.

(i) Isothermally Reacted Several pieces of the 7 mil sheet were vacuum-encapsulated in quartz tubes, solution annealed for 4 hours at 550°C in a vertical furnace, immediately transferred to a horizontal furnace at 350°C where they remained for 12 minutes, and then quenched in cold water. The encapsulation tubes were broken with pliers as they were submerged in water to facilitate quenching.

(ii) Quenched and Aged Discs of 2.3 and 3.0 mm diameter were punched from the sheet. These were solution annealed for 35 minutes

at 550°C in air in a vertical furnace and then immediately quenched in cold water. They were dried thoroughly and then aged for 30 minutes at 350°C in air, followed by another cold water quench.

2.3 Electropolishing

Both 2.3 and 3.0 mm discs were polished in a twin-jet Fishione apparatus using a 25% nitric acid - 75% methanol solution at around -30 to -40 °C. The voltage and current conditions varied for 2.3 and 3.0 mm foils, but were generally around 14-20 kV and 15-35 mA. After perforation, the thin foils were rinsed in three separate methanol baths and immediately dried and stored under vacuum.

2.4 Transmission Electron Microscopy

Typical contrast analyses were performed using Philips 301 and Siemens 102 microscopes, operating at 100 keV accelerating potentials. In general, bright field (BF) micrographs were taken in strong two-beam conditions with s>0. Weak-beam dark field (WBDF) images were obtained by tilting the incident illumination so that the desired diffracted beam was positioned on the optic axis (usually $\vec{g}$,$3\vec{g}$ conditions were used). Selected-area diffraction patterns were recorded using a 1 μm intermediate aperture in the Siemens 102, and a 10μm aperture in the Philips 301.

3. RESULTS

Since there is only a small difference in lattice parameters between γ'(metastable) and γ(Ag_2Al) precipitates, it is virtually impossible to distinguish between them in an electron diffraction pattern.[4] However, the heat treatments employed in this study are most likely to have produced either γ' or early-stage γ,[12] as designated in the following.

3.1 Edges of γ' Precipitate Plates

Figure 1(a) shows a γ' precipitate completely enclosed within a thin foil from the quenched and aged sample. The orientation is such that its face is perpendicular to the electron beam, i.e. zone axis $(\vec{B}) = [0001]_\gamma \; // [111]_{Al}$, as shown by the diffraction pattern in Fig. 1(b). Several important crystallographic directions are superimposed on the precipitate and six of its edges are numbered. These numbered edges are all parallel to <110> directions within the (111) matrix plane. Notice that the segments between the numbered edges appear macroscopically to follow <112> directions, however, ledges are apparent on all of these segments (arrows).

The nature of the ledges becomes apparent in the higher resolution BF-WBDF pair of micrographs in Fig. 2, taken between edges numbered 5 and 6 in Fig. 1(a), with $\vec{g} = [\bar{2}02]$. From these enlargements, it is clear that both the terraces and risers of the ledges into which the <112> edge is resolved are also parallel to <110> directions, in this particular case, to $[0\bar{1}1]$ and $[\bar{1}01]$. Also notice that in the WBDF micrograph, the contrast is intermittent and appears to be weakest along the $[\bar{1}01]$ edges, parallel to $\vec{g}$. Since many of the ledges are only about 25 Å high, there is obviously a strong preference for the edges to lie along close-packed <110> directions even on a very fine scale.[49] In addition, notice that as the interface deviates further away from the $[0\bar{1}1]$ direction, the density of ledges increases, while their height remains unchanged.

This precipitate was tilted through a large angle ($\sim 45°$) into an [013] zone axis to see if individual dislocations could be resolved

at locations along the edge where the contrast appeared to be coming from a single source, i.e. at positions 2 and 5 in Fig. 1(a) when $\vec{B}$ = [111]. Figure 3 shows the results of this experiment. It is apparent that the edges do include closely spaced dislocations. At least two or three are visible at locations A and B in this micrograph; however, there may be more dislocations which are not distinguished due to the limitations of this contrast mechanism.[50,51]

Figure 4 shows the results of contrast experiments performed on the precipitate plate as a whole. Two features are of particular interest: (1) contrast from around the plate edge or periphery, and (2) contrast from the linear defect across the center of the precipitate face. Note that images formed with the three different <220> reflections exhibit strong contrast around the plate edges, except for the edge segments parallel to $\vec{g}$. In addition, contrast reversals occur across portions of the edges as the sign of s is reversed (Figs. 4(a) and (b)). Such "line-of-no-contrast" behavior is typical of an edge dislocation loop, where the extra half-plane is normal to, and $\vec{b}$ is parallel to, the electron beam.[52,53] Under these conditions $\vec{g}.\vec{b}$ = 0 everywhere; however, contrast arises from displacements $\vec{R}_n$ normal to the slip plane, except again where $\vec{g}.\vec{R}_n$ = 0. This type of contrast can also occur for coherent or partially coherent plate-shaped precipitates,[52] which appears to be the situation for this γ' precipitate. The strain field at the plate edge in fact exhibits the contrast behavior typical of a 1/3[111] vacancy loop.[53] Notice that the "line-of-no-contrast" variation with $\vec{g}$ also occurs along the risers of the 25 Å ledges along the edge (Fig. 2).

Lastly, a contrast analysis of the dislocation across the diameter of the plate was performed. This dislocation is invisible for $\vec{g} = [1\bar{1}\bar{1}]$ and displays evidence of a double image when $\vec{g} = [2\bar{2}0]$, indicating that it is wrapped around the precipitate in a dipole configuration and has a Burgers vector $\vec{b} = 1/2[0\bar{1}1]$, rather than the more commonly observed 1/6 <112> type.[3,4] Such a dislocation may have been freshly adsorbed from the matrix, presumably dissociating shortly afterwards into the Shockley partials usually found on the broad faces of these plates.[1-4]

Figure 5 also shows a γ' precipitate whose broad face is oriented perpendicular to the electron beam, similar to the previous case. Although the complete contrast analysis is not shown, dislocations at location B on the left end of the precipitate are highly visible when $\vec{g} = [0\bar{2}2]$, but show reduced contrast and are invisible when $\vec{g} = [20\bar{2}]$ and $[2\bar{2}0]$, respectively. Most of the dislocations on the precipitate face as well as those on the right end at C display similar behavior, i.e. they are invisible for one value of $\vec{g}$. Again, comparison with the appropriate $\vec{g}.\vec{b}$ values indicates that these are Shockley partial dislocations on (111), primarily with $\vec{b} = 1/6[\bar{1}\bar{1}2]$ and $1/6[\bar{1}2\bar{1}]$. The somewhat random, tangled distribution is similar to that observed on the faces of "immature" precipitates plates by Laird and Aaronson.[4]

In particular, note how the one dislocation on the precipitate face at edge B (enlarged in Fig. 6(a)) appears to interact with the entire array of partial dislocations out to the periphery of the plate (arrow). This configuration suggests that it may be wrapped around the precipitate as a loop, similar to the dipole observed on the

precipitate in Figs. 1 through 4. This may also be true for other dislocations on the precipitate face.

Of special importance is the ledge on the right end of the precipitate (enclosed in box), also shown enlarged in Fig. 6(b). This 1400 Å ledge appears to be identical to the growth ledges or "superledges" on the edges of plates which contributed to the lengthening rate plotted in Fig. 10 of Laird and Aaronson.[8] However, the present contrast analysis shows that this "superledge" is actually an array of Shockley partial dislocations lying along <110> directions and that this array of partials serves as a set of ledges on the edge of the 1400 Å "superledge". Dislocations moving toward the precipitate edge appear to bend around the ledge corner as indicated by the arrows in Fig. 6.

3.2 Faces of γ' Precipitate Plates

Dislocation/ledge structures on the faces of several different precipitates were analyzed in the isothermally aged sample. Two separate contrast experiments were performed, the results of which are shown in Figs. 7 through 9.

Trace analyses of the precipitates in Fig. 7 show that the horizontal one lies on $(1\bar{1}\bar{1})$, while the nearly vertical precipitate has a (111) habit plane. In addition, the foil thickness is about 2900 Å, as estimated from either the projected length, or the number of extinction fringes in dislocations C and F when $\vec{g} = [\bar{1}11]$ and $s > 0$. This is sufficient for dynamical contrast conditions to apply.[52,53]

It is apparent from these micrographs that impingement of the horizontal precipitate has nucleated a profusion of ledges on the face

of the vertical precipitate, as observed for impinging precipitates in Al-Cu alloys.[18,54] Furthermore, notice that in this densely ledged region, the displacement fringes on the face of the precipitate bend almost 90° (white arrow) in the WBDF micrograph in Fig. 7(c), indicating a substantial change in precipitate thickness. The ledges are so closely spaced in this area that there is no hope of resolving them with the instrument used, even when WBDF is employed. Similarly, when contrast analyses are performed on ledges such as G, H, and H_1, the results reflect the contributions of overlapping strain fields from some number of very closely spaced dislocations. Hence, there is usually some uncertainty in the interpretation. In this particular case, however there are 1/2<110> matrix dislocations nearby at C, D, E and F; these can be used to help check the consistency of the results. When the contrast behavior of dislocations/ledges A, B, G, H and H_1 is analyzed, the resultant Burgers vectors are of the type $\vec{b} = 1/2[0\bar{1}1]$ and $\vec{b} = 1/2[\bar{1}10]$, since invisibility occurs when $\vec{g} = [\bar{1}11]$ and $[11\bar{1}]$, respectively. Because the basic ledge unit in this system is considered to be a 1/6 <112> Shockley partial dislocation,[1,3,4] these results indicate that clustering or alignment of the partial dislocations on alternate (111) planes is occuring, giving 1/2<110> contrast behavior. This in turn implies that Shockley partials of different sign must interact, otherwise the resultant strain field would give the appearance of some multiple of an isolated Shockley partial. In this case, both $1/2[0\bar{1}1]$ and $1/2[\bar{1}10]$ dislocations are present on the (111) plane, indicating that all three types of Shockley partials are interacting.

Another matrix dislocation at L displays the contrast behavior of a 1/2[011] dislocation lying in a $(1\bar{1}1)$ plane, where the upper portion of the dislocation appears to be intruding into the (111) interphase boundary as indicated by its alignment along the $[10\bar{1}]$ direction, parallel to the densely-packed ledges. Close inspection of the aligned portion of dislocation L in Figs. 7(a) and (c) also reveals evidence of a faint double image as though it might be slightly dissociated, and fringe displacements also occur along this segment. Therefore, incorporation of matrix or intruder dislocations also appears to be a possible misfit dislocation/ledge source in this system.[55] A similar situation seems to be occurring for the matrix dislocation immediately above ledge H_1.

The ledge height (h) at position H was estimated to be 16 Å from the fringe displacement in Fig. 7(c), using the following equation due to Gleiter:[56]

$$h = \sin(\beta) \sin(\phi)\, m \qquad (1)$$

where β= angle between the precipitate interface and the foil surface, ϕ= angle between the fringes and the ledge line direction and m = magnitude of the fringe shift. This is roughly double the height expected for the three dislocations visibly associated with this ledge as shown in Fig. 8, possibly indicating that additional, but unresolved ledges are also present.

Other than the densely ledged region near impingement, there are few interfacial dislocations on the vertical precipitate. The impinging precipitate on the other hand, has a regular two-dimensional and in some places, hexagonal interfacial dislocation network. This network

is similar to those on γ plates observed by Laird and Aaronson,[4] indicating that this particular plate may be a well-developed semicoherent precipitate, substantially further along in its evolution toward an equilibrium interfacial structure. Dislocations in the two-dimensional network are spaced an average of 550 Å apart, which is somewhat larger than the 200-400 Å spacing calculated for equilibrium precipitates,[4] indicating that this precipitate has not yet reached its equilibrium configuration.

Burgers vector determinations of dislocations I and K yield $\vec{b} = 1/6[\bar{1}12]$ and $\vec{b} = 1/6[21\bar{1}]$, respectively, while for J, $\vec{b} = 1/2[011]$. Dislocations J and K have similar orientations, though, possibly indicating that multiple dislocation/ledge interactions are occurring on this interface as well. In addition, fringe displacements only occur across dislocations near to the edge, indicating that either some of the dislocations are not associated with ledges, i.e. they are 1/2 <110> misfit dislocations, or that the ledges are multiples of three partial dislocations high, so closely spaced that they are not individually resolvable and do not produce a phase shift, i.e. $\alpha = \vec{g}.\vec{R}_n = 2\pi$ [3,52]

Trace analyses of the precipitates in Fig. 9 show that they also lie on $(1\bar{1}\bar{1})$. Burgers vector analyses of the dislocations/ledges on these precipitates indicate that they are mainly Shockley partials with $\vec{b} = 1/6[\bar{1}2\bar{1}]$ and $1/6[2\bar{1}\bar{1}]$, since they are invisible when $\vec{g} = [\bar{1}11]$ and $\vec{g} = [\bar{1}11]$ and $[0\bar{2}0]$, respectively. In addition, fringe reversals and disappearances occur across many of the dislocations, i.e. B, D, E, F and B_1 in Fig. 9(c), further verifying their 1/6<112> nature.[3,52]

However, as in the previous analyses, these Shockley partials appear to be interacting, giving the contrast behavior of dislocations with 1/2<110> Burgers vectors, as evidenced by A, C and A_1 in Figs. 9(a) and (b), which are visible and display evidence of double images when $\vec{g} = [\bar{2}\bar{2}0]$.

Another interesting feature apparent from this series of micrographs is that dislocations on opposite faces of the precipitates show a strong tendency to align vertically above one another. This effect is clearly evident in the enlargement in Fig. 10, where pairs of dislocations on opposite faces are indicated. Such alignment suggests the presence of loops around the precipitates. One possible explanation for the occurrence of these loops is that when precipitates are thin, as these appear to be, dislocations on opposite faces may preferentially align in order to reduce their strain energy.[57,58] Further, when these aligned dislocations reach the precipitate edges, their screw components may combine to reduce their line length and form vacancy/interstitial pairs of loops as suggested by Dahmen and Westmacott,[59] where the vacancy loop is left wrapped around the precipitate to accommodate misfit in the plane of the precipitate, and the interstitial loop glides into the matrix. Dislocations were occasionally observed to emanate from the ends of precipitates in this sample, indicating that such loop formation may have been occurring.

4. DISCUSSION

While the results of this study are in general agreement with those of previous investigations,[1,3,4] several new observations were made. Possibly the most striking observation was the prevalence of

1/2<110> dislocation contrast on the precipitate faces. In addition, two types of 1/2 <110> contrast were apparent: (1) that which was positively associated with ledges and therefore, was probably due to interacting 1/6 <112> dislocations/ledges on alternate {111} planes, i.e. G and H in Fig. 7, and (2) that which did not appear to be associated with a ledge and was thus due to 1/2<110> misfit dislocations, i.e. the dislocation across the face in Fig. 1(a). While only a few of the latter type dislocations were seen, nearly half of the interfacial dislocations/ledges on the precipitate faces appeared to be composed of interacting 1/6 <112> partials, indicating a strong tendency for diffusional and/or elastic interaction. These findings agree with the models for ledge growth developed by Jones and Trivedi,[40] which predict multiple-ledge interactions. Such combining of ledges may also be responsible for the anomalous migration rates of some interfacial ledges observed by Laird and Aaronson.[8] In addition, the contrast analyses showed that all three variants of Shockley partial dislocations may be present on alternate {111} planes. Nucleation of all three variants may be a favorable way for the precipitate to reduce the overall strain energy associated with the fcc-hcp transformation, by reducing the elastic distortion in the matrix at the precipitate edges.[58]

There also appeared to be a strong tendency for all aspects of the precipitate interface to lie along low-energy <110> directions. This includes dislocations and ledges on the precipitate faces as well as the edges of the precipitates. This effect was observed even for ledges on the edges only 25 Å high. In addition, there appeared to be a preference for dislocations/ledges on opposite faces of the

precipitates to align vertically. While this may be to reduce their interaction energy, it could also be associated with the formation of loops and accommodation of misift as discussed previously.

Lastly, it is important to recognize the structural similarity between ledges on the broad faces of the precipitates, and ledges on the edges of the same precipitates. Both lie along <110> directions, have Shockley partial dislocation character and are responsible for atomic transfer across the interface by a kink mechanism, which is shown schematically in Fig. 11. Notice the greater "free volume" associated with such a kink when compared to the remaining dislocation line, lying along <110>. The additional disorder introduced by a kink should make it a preferred site for atomic transfer across the interface and hence, explain why ledges on both the faces and edges of precipitates prefer to migrate by the motion of kinks parallel to the dislocation line direction, rather than by overall forward propagation of the dislocation ledge.

Furthermore, ledges on the broad faces of precipitates often deviate significantly from exact <110> orientations during the early stages of growth, i.e. refer to Fig. 5, and thus, should possess an abundance of kinks for growth. In this case, the kinks represent regions of disorder for easy transfer of solute across what is otherwise, a largely ordered interface. However, as a Shockley partial dislocation on the face of a precipitate travels toward the edge, it becomes constrained to lie along <110> due to the influence of other dislocations at the precipitate edge. Propagation of the edge now involves the cooperative motion of all these dislocations, and the agglomeration of kinks into

"superledges" such as those observed by Laird and Aaronson[8] presumably occurs as a result of diffusional and to a lesser extent elastic intractions between kinks, similar to the motion of interacting steps as treated by Jones and Trivedi.[40]

It should be emphasized that relaxations are not accounted for in the hard-sphere model shown in Fig. 11 and therefore, the actual interface is probably somewhat different. However, even considering relaxations the edge of a kink should still be a preferred site for advancement of the interface.

5. CONCLUSIONS

(1) The present work indicates that growth (thickening) of precipitates occurs by lateral migration of 1/6 <112> Shockley partial dislocations/ledges along the precipitate faces, in agreement with previous investigations.

(2) Misfit 1/2 <110> dislocations were also observed on the faces of these precipitates, although less frequently than 1/6 <112> dislocations.

(3) Nucleation of all three variants of Shockley partials on alternate {111} planes appears to occur at times, possibly due to a reduction in the overall strain energy associated with the fcc-hcp transformation.

(4) There is a strong tendency for different variants of single 1/6 <112> dislocation ledges on alternate {111} planes to interact, forming multiple-unit ledges which display the contrast behavior of 1/2 <110> dislocations. Although 1/3 <111> dislocation contrast was not observed for interacting ledges in this study, there seems to be

no reason preventing its occurrence if the proper combination of Shockley partials interact. However, this is less favorable from strain energy considerations.

(5) Both the edges of precipitates, and ledges on the edges, are composed of 1/6 <112> partial dislocations, which align vertically or slightly behind one another along the precipitate periphery.

(6) There is a strong tendency for dislocations/ledges on both the faces and edges of the precipitates to lie along low-energy <110> directions. In addition, ledges on opposite faces of precipitates often align vertically, and there is evidence that some of the dislocations on precipitate faces may be loops, wrapped around the precipitates in a dipole configuration.

(7) There is a vacancy-type strain field at the edges of precipitate plates, and the density of ledges on the precipitate edges increases as the edges deviate further from a <110> direction.

(8) Ledges nucleate at precipitate intersections and by incorporation of matrix dislocations into the interface of γ' precipitates, in addition to nucleation at plate edges as observed in previous investigations.

(9) Ledges on both the faces and edges of precipitate plates may prefer to migrate by the motion of kinks parallel to the dislocation line direction rather than by overall forward propagation of the dislocation ledge due to additional disorder introduced by a kink, making it a preferred site for atomic transfer across the interface.

ACKNOWLEDGEMENTS

The authors thank U. Dahmen for many helpful discussions concerning

ledge growth. This work was supported by the Director, Office of Energy Research, Office of Basic Energy Sciences, Materials Sciences Division of the U.S. Department of Energy under Contract No. DE-AC03-76SF00098. One of the authors (J.M. Howe) acknowledges partial support by National Science Foundation Grant No. DMR-81-19507 through the Carnegie-Mellon University Metals Research Laboratory, and support to H.I. Aaronson from this same source is also gratefully acknowledged.

REFERENCES

1. R. B. Nicholson and J. Nutting, Acta Met. 9, 250 (1961).
2. G.R. Frank, D.L. Robinson and G. Thomas, J. Appl. Phys. 32(1), 1763 (1961).
3. J.A. Hren and G. Thomas, Trans. Met. Soc. AIME 227, 308 (1963).
4. C. Laird and H.I. Aaronson, Acta Met. 15, 73 (1967).
5. J.B. Clark, in High Temperature, High-Resolution Metallography, p. 347, Gordon and Breach (1969).
6. H.I. Aaronson and J.B. Clark, Acta Met. 16, 845 (1968).
7. H.I. Aaronson, J.B. Clark and C. Laird, Met. Sci. J. 2, 155 (1968).
8. C. Laird and H.I. Aaronson, Acta Met. 17, 505 (1969).
9. Y.C. Liu and H.I. Aaronson, Acta Met. 18, 845 (1970).
10. K. Abbott and C.W. Hawarth, Acta Met. 21, 251 (1973).
11. H.I. Aaronson, K.C. Russell and G.W. Lorimer, Met. Trans. 8A, 1644 (1977).
12. C.S. Barrett, A.H. Geisler and R.F. Mehl, Trans. Met. Soc. AIME 143, 134 (1941).
13. H.I. Aaronson, in Decomposition of Austenite by Diffusional Processes, p. 387, Interscience Publishers (1962).
14. C. Laird and H.I. Aaronson, Trans. Met. Soc. AIME 242, 1393 (1968).
15. C. Laird and H.I. Aaronson, Trans. Met. Soc. AIME 242, 1437 (1968).
16. H.I. Aaronson, C. Laird and K.R. Kinsman, in Phase Transformations, p. 313, ASM, Metals Park, OH (1970).
17. H.I. Aaronson, J. Microscopy 102(3), 275 (1974).
18. R. Sankaran and C. Laird, Acta Met. 22, 957 (1974).
19. M. Ferrante and R.D. Doherty, Scripta Met. 10, 1059 (1976).

20. Y.H. Chen and R.D. Doherty, Scripta Met. 11, 725 (1977).

21. H.I. Aaronson, Scripta Met. 11, 731 (1971).

22. R.D. Doherty, M. Ferrante and Y.H. Chen, Scripta Met. 11, 733 1977.

23. H.I. Aaronson, Scripta Met. 11, 741 (1977).

24. H.I. Aaronson, Trans. Indian Inst. Metals 32(1), 1 (1979).

25. M. Ferrante and R.D. Doherty, Acta Met. 27, 1603 (1979).

26. K.E. Rajab and R.D. Doherty, in Proceedings of an International Conference on Solid-Solid Phase Transformations, p. 101, The Met. Soc. AIME, Warrendale, PA (1982).

27. C. Zener, J. Appl. Phy. 20, 950 (1949).

28. R.F. Mehl and C.A. Dube, in Phase Transformations in Solids, p. 545, John Wiley, New York (1951).

29. F.S. Ham, Quart. Appl. Math 17, 137 (1959).

30. G. Horvay and J.W. Cahn, Acta Met. 9, 695 (1951).

31. G. Thomas and M.J. Whelan, Phil. Mag. 6(2), 1103 (1961).

32. L. Kaufman, S.V. Radcliffe and M. Cohen, in Decomposition of Austenite by Diffusional Processes, p. 313, Interscience Publisher (1962).

33. C. Zener, Trans. Met. Soc. AIME 167, 550 (1967).

34. C. Atkinson, Acta Met. 16, 1019 (1968).

35. R. Trivedi, Met. Trans. 1, 921 (1970).

36. R. Trivedi, Acta Met. 18, 287 (1970).

37. G.J. Jones and R. Trivedi, J. Appl. Phy. 42, 4299 (1971).

38. C. Atkinson, H.B. Aaron, K.R. Kinsman and H.I. Aaronson, Met. Trans. 4, 783 (1973).

39. W.P. Bosze and R. Trivedi, Met. Trans. 5, 511 (1974).

40. G.J. Jones and R. Trivedi, J. Cryst. Growth 29, 155 (1975).

41. M. Hillert, Met. Trans. 6A, 5 (1975).

42. E.P. Simonen and R. Trivedi, Acta Met. 25, 945 (1977).

43. C. Atkinson, Proc. Roy. Soc. London A378, 351 (1981).

44. P. Merle and E. Fouquet, Acta Met. 29, 1919 (1981).

45. P. Merle and J. Merlin, Acta Met. 29, 1929 (1981).

46. R. Trivedi, in Proceedings of an International Conference on Solid-Solid Phase Transformations, p. 477, The Met. Soc. AIME, Warrendale, PA (1982).

47. R.D. Doherty and B. Cantor, in Proceedings of an International Conference on Solid-Solid Phase Transformations, p. 547, The Met. Soc. AIME, Warrendale, PA (1982).

48. M. Enomato, H.I. Aaronson, J. Avila and C. Atkinson, in Proceedings of an International Conference on Solid-Solid Phase Transformations, p. 567, The Met. Soc. AIME, Warrendale, PA (1982).

49. J.W. Christian, The Theory of Transformations in Metals and Alloys, p. 142, Pergamon Press, Oxford (1965).

50. D.J. Cockayne, I.L.F. Ray and M.J. Whelan, Phil. Mag. 20, 1265 (1969).

51. J.B. VanderSande, in Introduction to Analytical Electron Microscopy, p. 535, Plenum Press, New York and London (1979).

52. Sir P. Hirsch, A. Howie, R.B. Nicholson, D.W. Pashley and M.J. Whelan, Electron Microscopy of Thin Crystals, p. 260, 334, 245, 251, Robert E. Krieger Pub. Co., Malabar, FL (1977).

53. M.H. Loretto and R.E. Smallman, Defect Analysis in Electron Microscopy, p. 75, 45, Chapman and Hall, London (1975).

54. G.C. Weatherley, Can. Met. Quart. 8(2), 105 (1969).

55. G.C. Weatherley and R.B. Nicholson, Phil. Mag. 17, 801 (1968).

56. H. Gleiter, Acta Met. 17, 565 (1969).

57. W.T. Reed, Dislocations in Crystals, p. 128, McGraw-Hill, New York (1953).

58. A. Kelly and G.W. Groves, Crystallography and Crystal Defects, p. 220, Addison-Wesley, Reading (1970).

59. U. Dahmen and K.H. Westmacott, Phys. Stat. Sol. (A) 80, 249 (1983).

FIGURE CAPTIONS

Fig. 1 (a) Crystallographic features of γ' precipitate plate oriented perpendicular to the electron beam, and (b) corresponding electron diffraction pattern.

Fig. 2 BF-WBDF pair showing ledges lying along <110> directions at precipitate edge.

Fig. 3 WBDF micrograph showing closely spaced dislocations (arrows) around periphery of precipitate plate.

Fig. 4 Contrast analysis of γ' precipitates; (a)-(c) [111] orientation, (d)-(f) [101] orientation.

Fig. 5 Interfacial dislocations/ledges at the edges and on the face of a γ' precipitate plate; [111] orientation.

Fig. 6 Enlargements from Fig. 5 showing dislocation ledges on the precipitate face: (a) interacting with partial dislocations out to the plate edge (arrow), and (b) aligning (arrows) to become part of a "superledge" at the edge.

Fig. 7 Contrast analysis of two intersecting precipitates in the isothermally aged sample; [101] orientation.

Fig. 8 Enlargement from Fig. 7(a) showing three closely spaced dislocations associated with ledge H.

Fig. 9 Second contrast analysis of ledges on γ' precipitate faces; (a) [001] orientation, (b),(c) $[1\bar{1}2]$ orientation.

Fig.10 Enlargement from Fig. 9(a) showing alignment of dislocations on opposite faces of precipitates.

Fig. 11. Atomic model of a single atom kink in a Shockley partial dislocation ledge lying along <110>. Note the open space associated with the kink; paper normal is <111>.

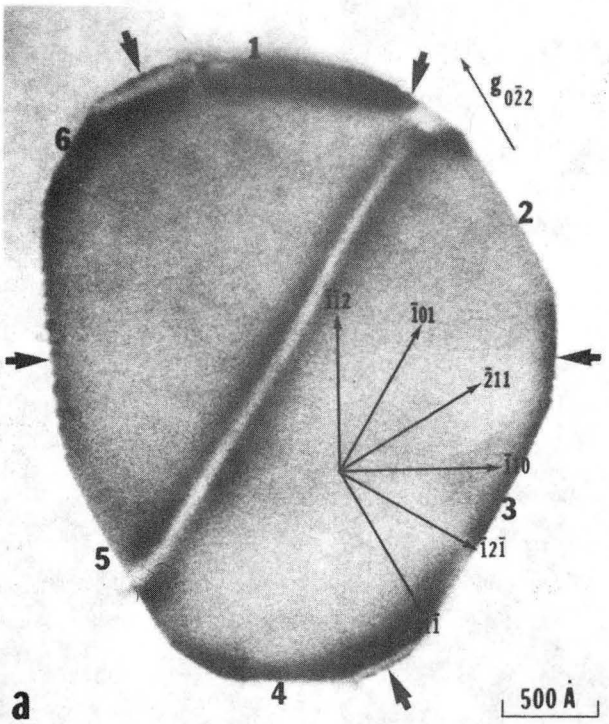

a

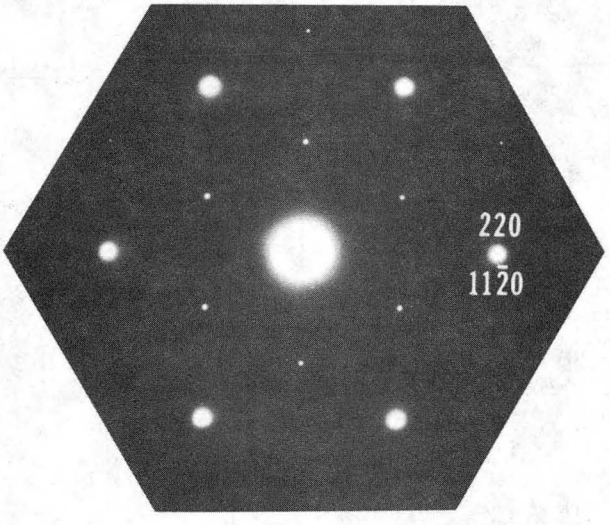

b $[111]_{Al} \parallel [0001]_{\gamma}$

XBB 838-6693A

Fig. 1

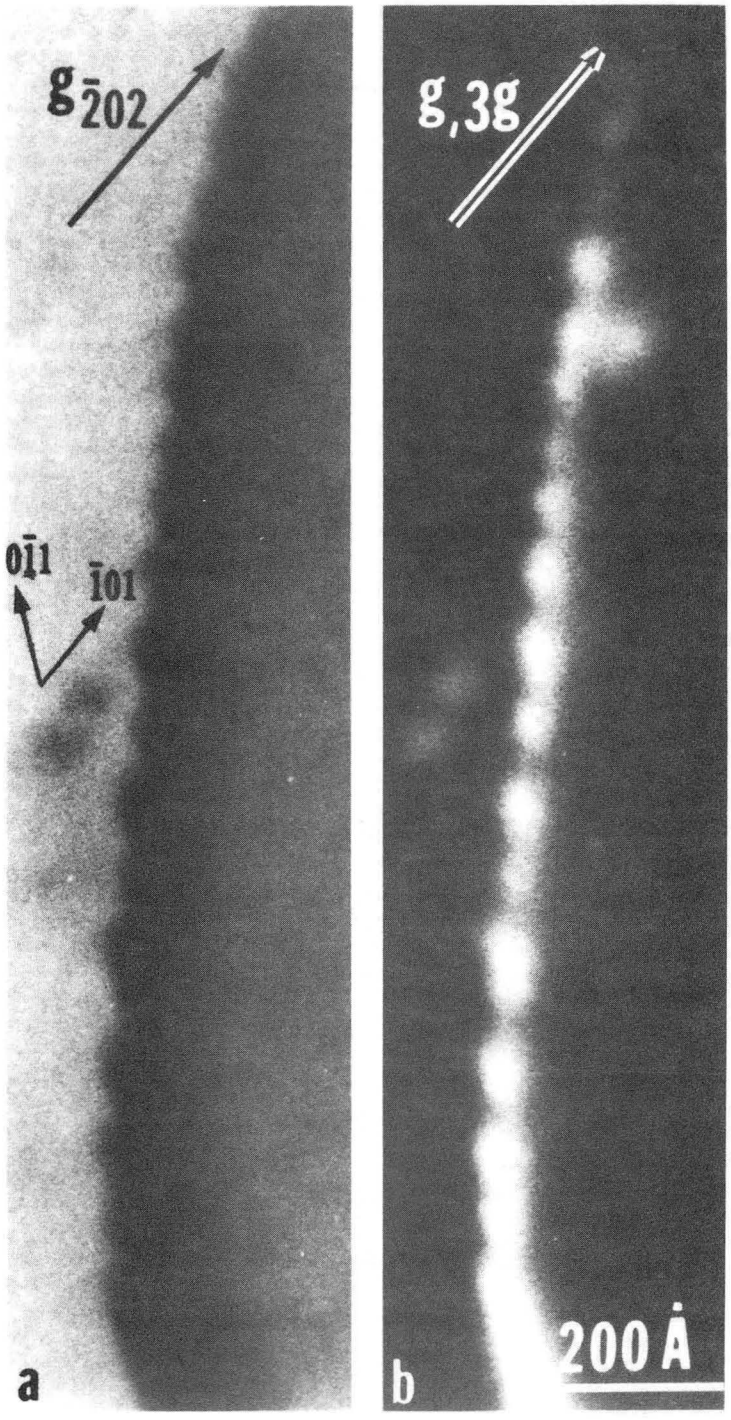

XBB 838-6701A

Fig. 2

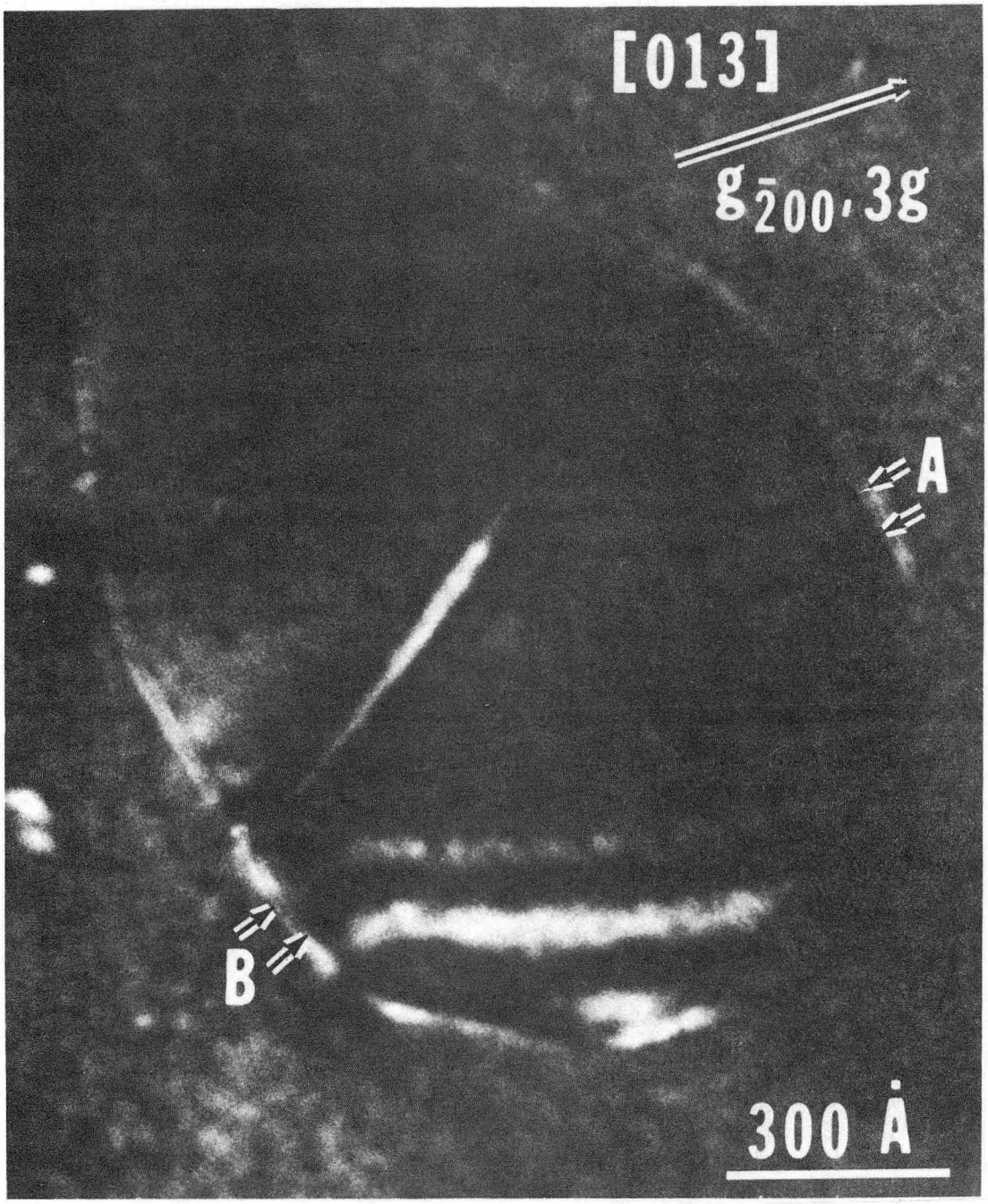

XBB 841-461

Fig. 3

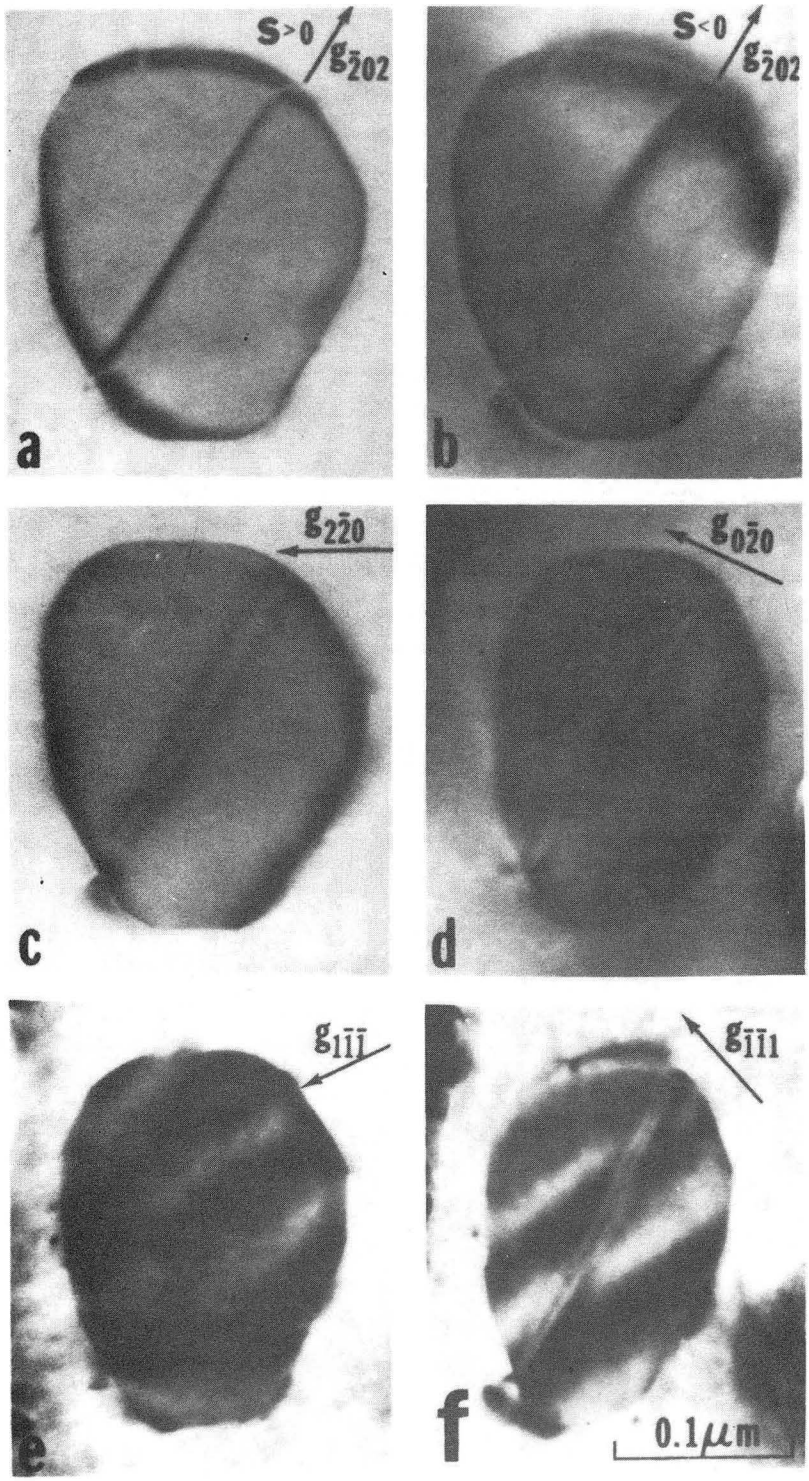

XBB 837-6707A

Fig. 4

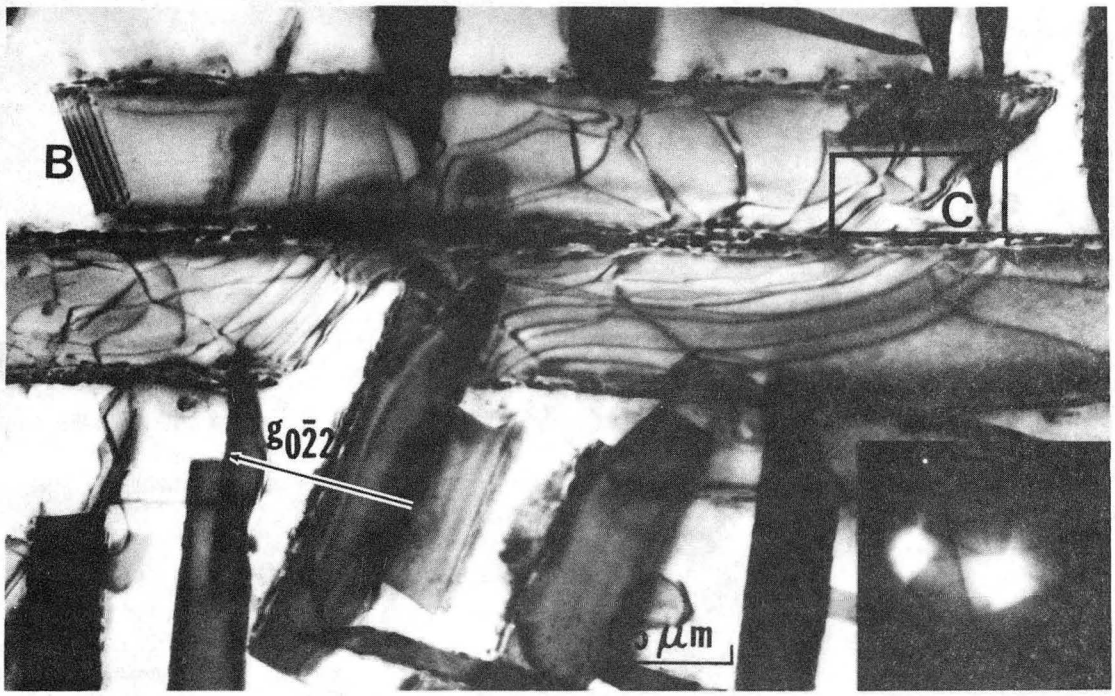

XBB 839-8362

Fig. 5

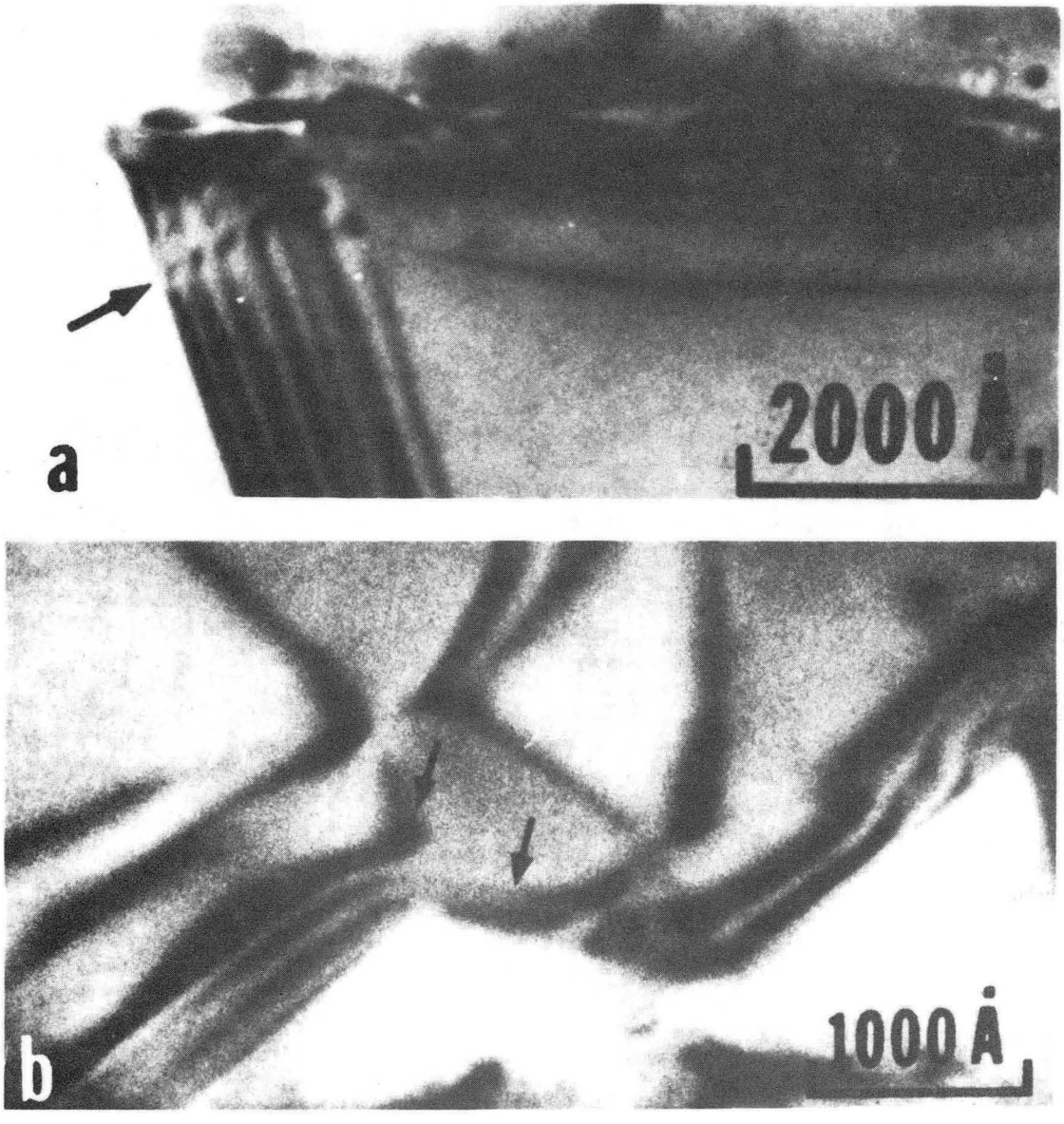

XBB 832-978A

Fig. 6

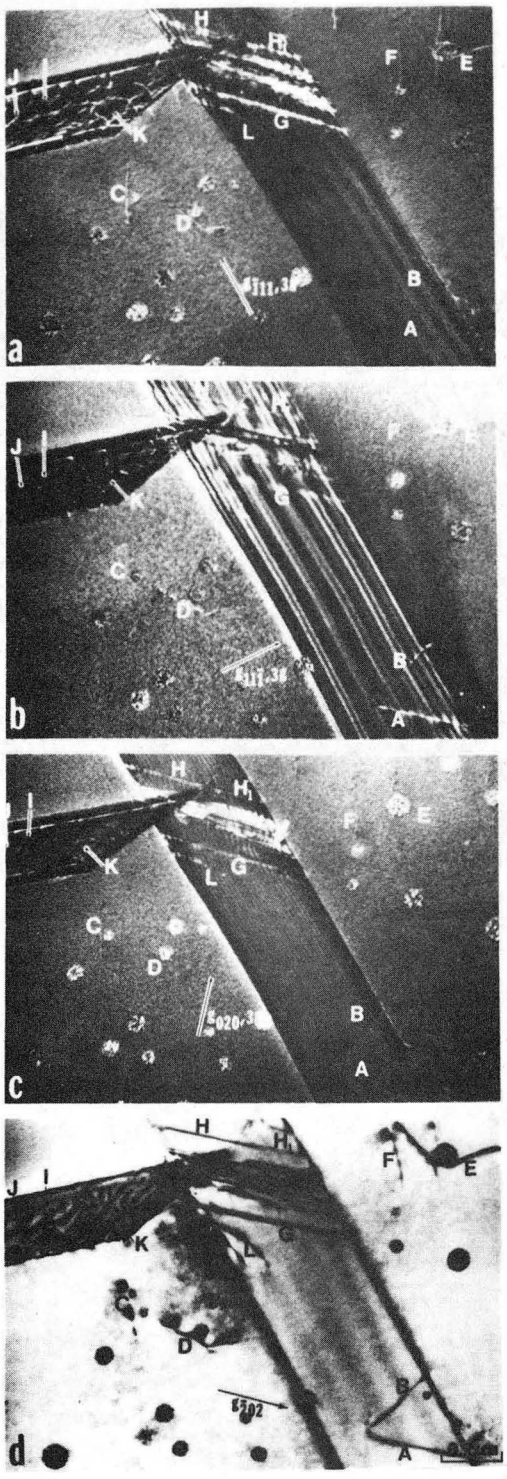

XBB 837-6709A

Fig. 7

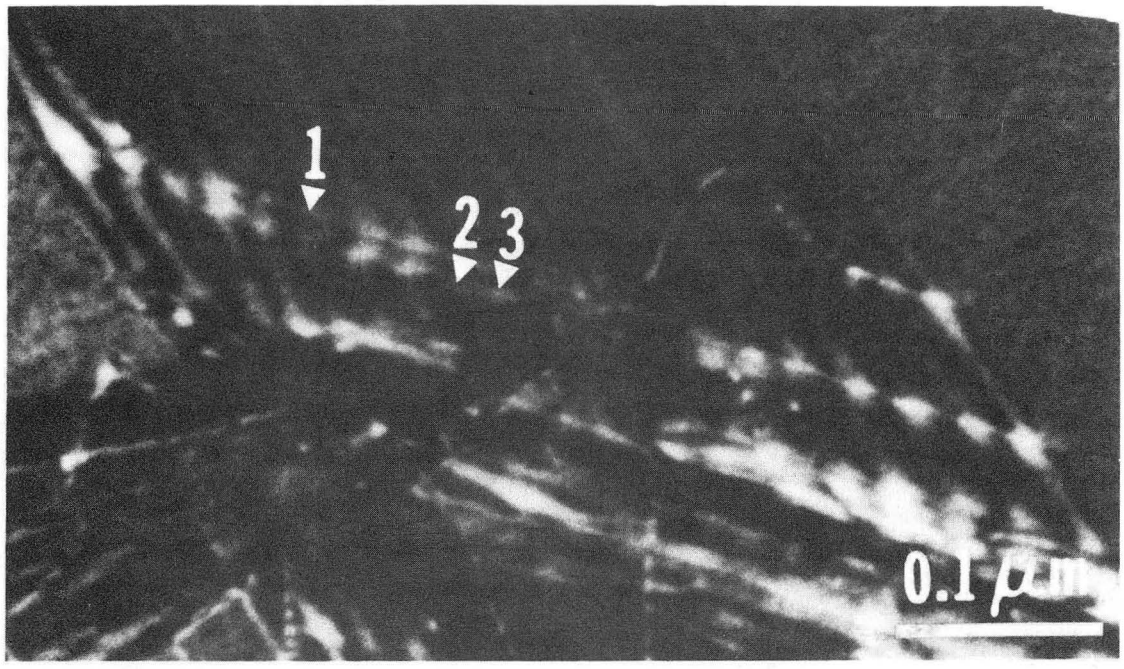

XBB 839-8361

Fig. 8

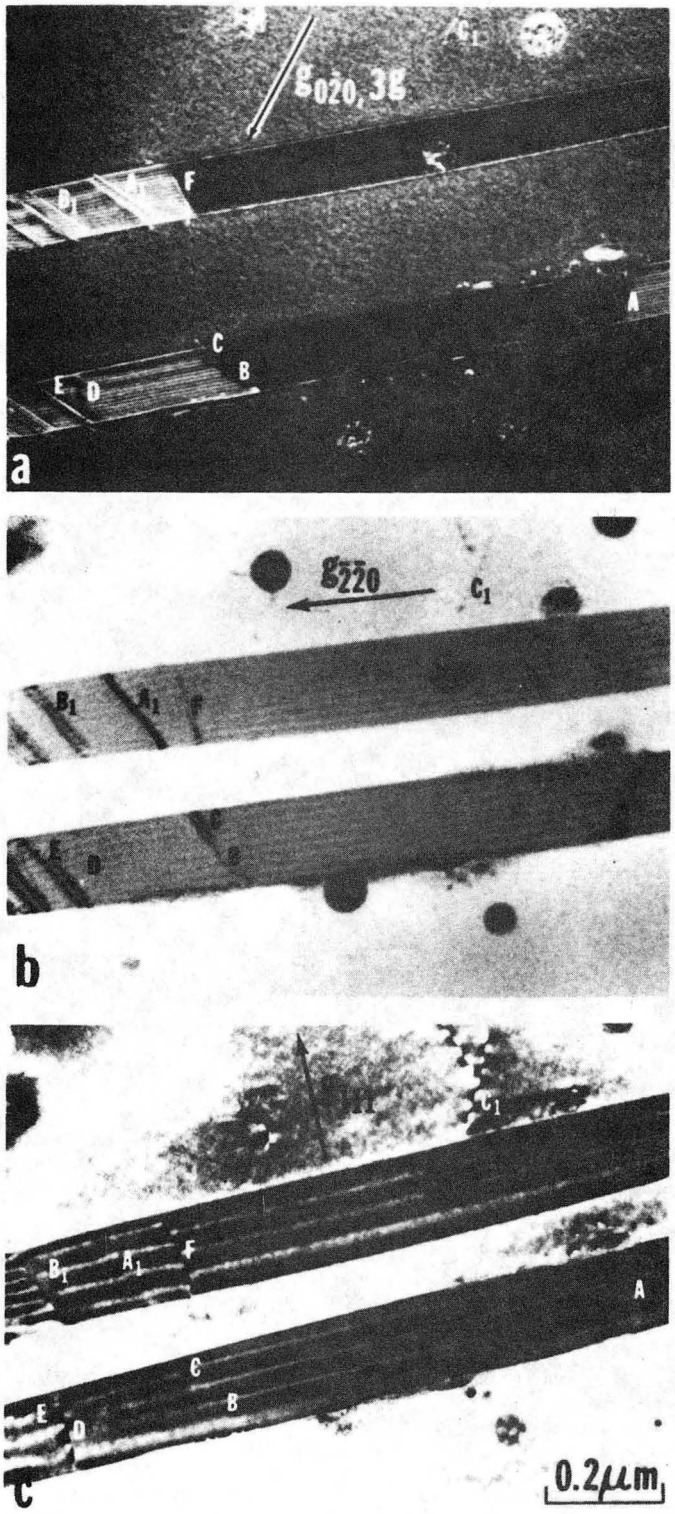

XBB 837-6705A

Fig. 9

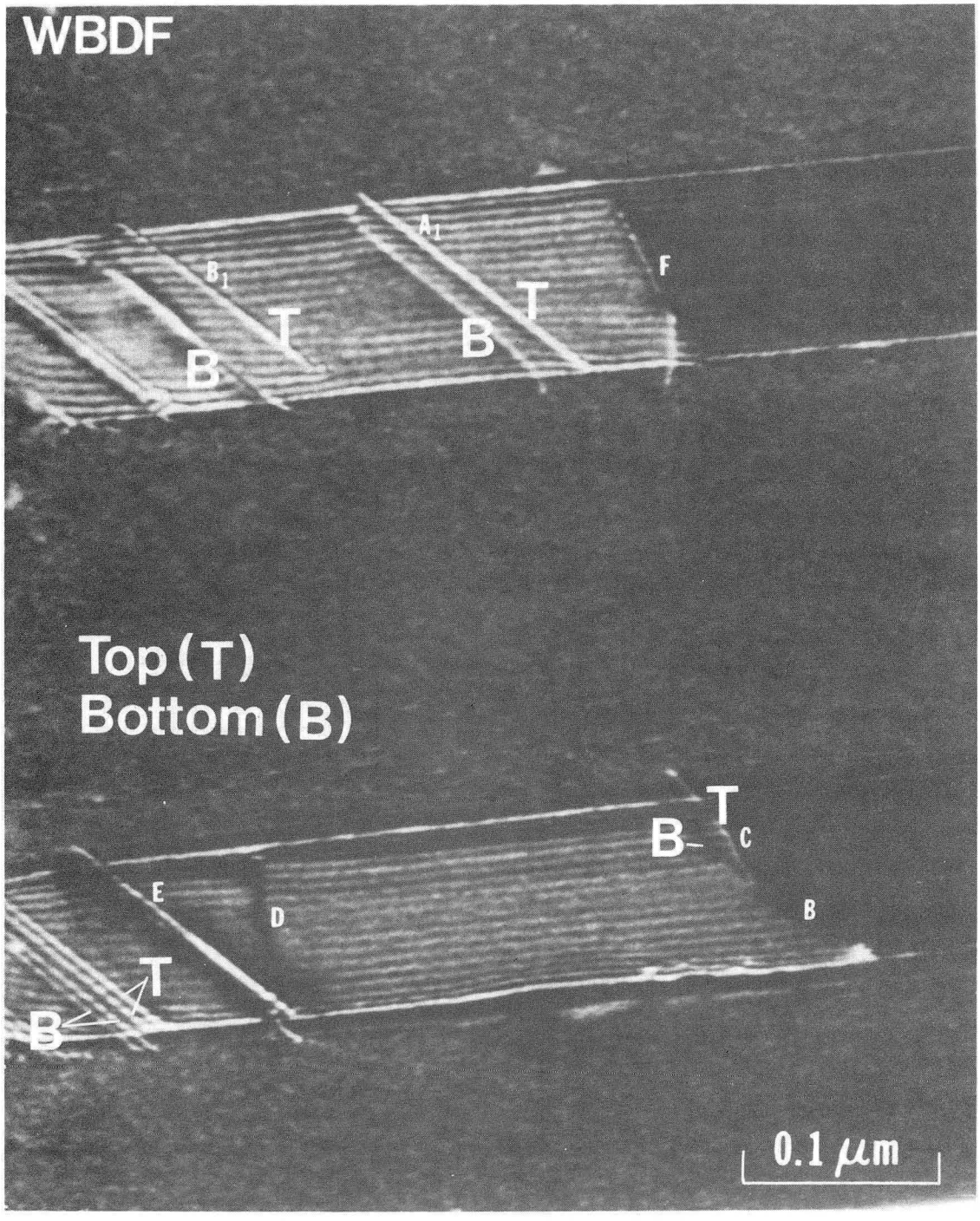

XBB 832-1601

Fig. 10

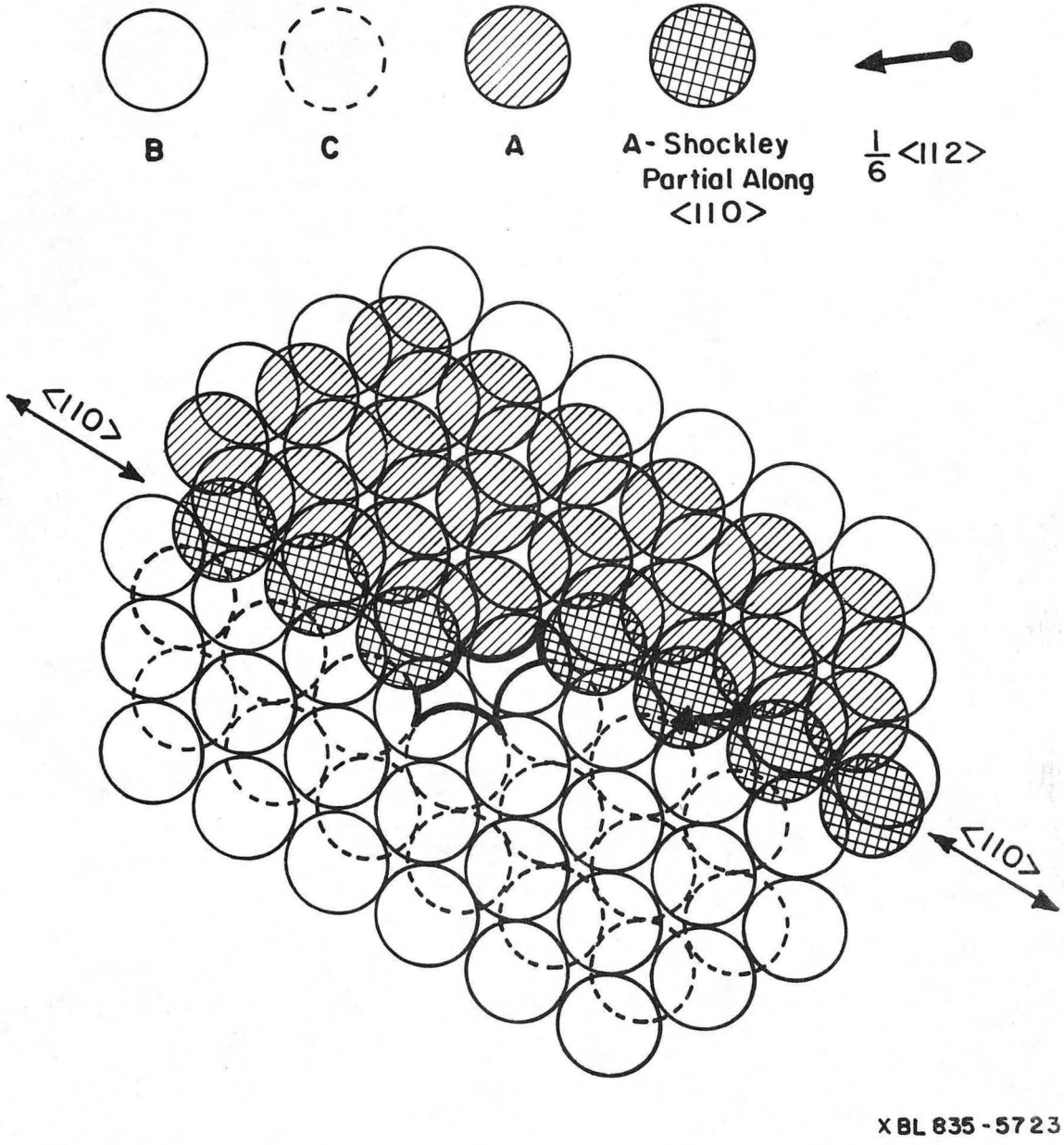

Fig. 11

This report was done with support from the Department of Energy. Any conclusions or opinions expressed in this report represent solely those of the author(s) and not necessarily those of The Regents of the University of California, the Lawrence Berkeley Laboratory or the Department of Energy.

Reference to a company or product name does not imply approval or recommendation of the product by the University of California or the U.S. Department of Energy to the exclusion of others that may be suitable.

TECHNICAL INFORMATION DEPARTMENT
LAWRENCE BERKELEY LABORATORY
UNIVERSITY OF CALIFORNIA
BERKELEY, CALIFORNIA 94720